

1 **Viral lysis alters the optical properties and biological availability of**  
2 **dissolved organic matter derived from picocyanobacteria**

3 ***Prochlorococcus***

4 **Xilin Xiao<sup>1</sup>, Weidong Guo<sup>1</sup>, Xiaolin Li<sup>1</sup>, Chao Wang<sup>1</sup>, Xiaowei Chen<sup>1</sup>, Xingqin Lin<sup>2</sup>,**

5 **Markus G. Weinbauer<sup>3</sup>, Qinglu Zeng<sup>2,4</sup>, Nianzhi Jiao<sup>1\*</sup>, Rui Zhang<sup>1\*</sup>**

6 1. State Key Laboratory of Marine Environmental Science, College of Ocean and Earth

7 Sciences, Fujian Key Laboratory of Marine Carbon Sequestration, Xiamen University,

8 Xiamen, China

9 2. Division of Life Science, The Hong Kong University of Science and Technology, Clear

10 Water Bay, Hong Kong, China

11 3. Sorbonne Universités, UPMC, Université Paris 06, CNRS, Laboratoire

12 d'Océanographie de Villefranche (LOV), Villefranche-sur-Mer, France

13 4. Department of Ocean Science, The Hong Kong University of Science and Technology,

14 Clear Water Bay, Hong Kong, China

15

16 \*Corresponding author: Nianzhi Jiao ([jjiao@xmu.edu.cn](mailto:jjiao@xmu.edu.cn)) or Rui Zhang

17 ([ruizhang@xmu.edu.cn](mailto:ruizhang@xmu.edu.cn))

18

19 **Competing interests**

20 The authors declare no competing interests.

21 **Abstract**

22 Phytoplankton contribute almost half of the world's total primary production. The  
23 exudates and viral lysates of phytoplankton are two important forms of dissolved  
24 organic matter (DOM) in aquatic environments and fuel heterotrophic prokaryotic  
25 metabolism. However, the effect of viral infection on the composition and biological  
26 availability of phytoplankton-released DOM is poorly understood. Here, we  
27 investigated the optical characteristics and microbial utilization of the exudates and  
28 viral lysates of the ecologically important unicellular picophytoplankton  
29 *Prochlorococcus*. Our results showed that *Prochlorococcus* DOM produced by viral lysis  
30 (Pro-vDOM) with phages of three different morphotypes (myovirus P-HM2, siphovirus  
31 P-HS2 and podovirus P-SSP7) had higher humic-like fluorescence intensities, lower  
32 absorption coefficients and higher spectral slopes compared to DOM exuded by  
33 *Prochlorococcus* (Pro-exudate). The results indicate that viral infection altered the  
34 composition of *Prochlorococcus*-derived DOM and might contribute to the pool of  
35 oceanic humic-like DOM. Incubation with Pro-vDOM resulted in a greater dissolved  
36 organic carbon (DOC) degradation rate and decreases in the absorption spectral slope  
37 and heterotrophic bacterial growth rate compared to incubation with Pro-exudate,  
38 suggesting that Pro-vDOM was more bioavailable compared to Pro-exudate. In  
39 addition, the stimulated microbial community succession trajectories were  
40 significantly different between the Pro-exudate and Pro-vDOM treatments, indicating  
41 that viral lysates play an important role in shaping the heterotrophic bacterial  
42 community. Our study demonstrated that viral lysis altered the chemical composition

43 and biological availability of DOM derived from *Prochlorococcus*, which is the  
44 numerically dominant phytoplankton in the oligotrophic ocean.

45 **Importance**

46 The unicellular picocyanobacterium *Prochlorococcus* is the numerically dominate  
47 phytoplankton in the oligotrophic ocean, contributing to the vast majority of marine  
48 primary production. *Prochlorococcus* releases a significant fraction of fixed organic  
49 matter into surrounding environment and supports a vital portion of heterotrophic  
50 bacterial activity. Viral lysis is an important biomass loss process of *Prochlorococcus*.  
51 Yet little is known about whether and how viral lysis affects *Prochlorococcus*-released  
52 dissolved organic matter (DOM). Our paper shows that viral infection alters the optical  
53 properties (such as the absorption coefficients, spectral slopes and fluorescence  
54 intensities) of released DOM and might contribute to a humic-like DOM pool and  
55 carbon sequestration in the ocean. Meanwhile, viral lysis also releases various  
56 intracellular labile DOM including amino acids, protein-like DOM and lower-molecular  
57 weight DOM, increases the bioavailability of DOM and shapes the successive trajectory  
58 of the heterotrophic bacterial community. Our study highlights the importance of  
59 viruses in impacting the DOM quality in the ocean.

## 60 Introduction

61 As the base of the marine food web, phytoplankton account for less than 1% of  
62 the photosynthetic biomass on Earth but contribute to almost half of the world's total  
63 primary production (1, 2). Large amounts of photosynthetically fixed organic matter  
64 are released into the surrounding seawater (3-5). It has been suggested that the rates  
65 of dissolved organic matter (DOM) production by phytoplankton will increase due to  
66 warmer, more acidic and more stratified conditions in the future ocean (6). Exudates  
67 and viral lysates are the two major sources of DOM released from phytoplankton. A  
68 significant proportion of phytoplankton are infected and lysed by viruses (5, 7, 8), thus  
69 releasing their cellular contents into the environment. Viral infections have been  
70 shown to restructure the fatty acids composition of *Emiliana huxleyi* (9). The  
71 production of DOM released by *Micromonas pusilla* was stimulated by viral infection,  
72 coupling with the change of DOM composition (4). Phytoplankton-derived DOM is  
73 highly bioavailable (10-12) and includes carbohydrates, amino acids (peptides and  
74 protein), carboxylic acids, lipids, and other cellular materials (such as pigments,  
75 polyphenols and trace metals) (3, 13-16). This DOM is primarily consumed by  
76 heterotrophic bacterioplankton, shapes the surrounding bacterial community  
77 structure and supports the function of the microbial loop (5, 17-20). Recently, Fang  
78 and colleagues (21) found that *Synechococcus* viral lysate may play a role as a source  
79 of organic nitrogen to regulate the transcription of the N-metabolism related genes of  
80 uninfected co-occurring phytoplankton.

81 In tropical and subtropical oligotrophic oceans, the unicellular

82 picocyanobacterium *Prochlorococcus* is the numerically dominant phytoplankton (22).  
83 Its specific divinyl-chlorophyll *a* accounts for 30–60% of the total chlorophyll *a* in  
84 subtropical oligotrophic oceans (23). Data from field surveys indicate that virus-  
85 mediated mortality is responsible for up to 60% of *Prochlorococcus* cell loss (8, 24, 25)  
86 and releases various DOM that serves as a large bioavailable carbon source in the vast  
87 oligotrophic oceans. It is estimated that *Prochlorococcus* releases 9-24% of its daily  
88 primary productivity as DOM into the surrounding environment, which supports a  
89 large part of bacterial production in oligotrophic regions (3). The chemical molecular  
90 analysis showed that the released DOM consists of low-molecular weight (LMW)  
91 carboxylic acids, hydrocarbon, amino acids as well as small, nonpolar materials (3, 26,  
92 27). However, the detailed effects of virus infection on the composition and microbial  
93 utilization of DOM released from *Prochlorococcus* remain unstudied.

94 *Prochlorococcus* MED4 is an ecologically important high light-adapted  
95 *Prochlorococcus* model strain. MED4 is distributed in the upper-middle euphotic zone  
96 and achieves numerical dominance in well-mixed, nutrient-rich, high-latitude waters  
97 (28). In this study, we conducted a microcosm experiment with DOM exuded by  
98 *Prochlorococcus* during growing (Pro-exudate) and DOM released by lysis of  
99 *Prochlorococcus* cells (Pro-vDOM) with infection of three lytic phages (myovirus P-HM2,  
100 siphovirus P-HS2, and podovirus P-SSP7). We investigated the optical properties and  
101 bioavailability of these different DOM types and the response of the microbial  
102 community to a low dose of Pro-vDOM. In recent decades, it was demonstrated that  
103 the absorption and fluorescence properties of DOM provide powerful indexes of DOM

104 characteristics (29), and they have been widely used in oceanographic studies (30, 31).  
105 The chemical composition of phytoplankton-derived DOM has been studied in detail  
106 using different mass spectrometry analyses (13, 15, 27). However, it is difficult to  
107 connect such analyses with oceanographic surveys that target the optical  
108 characteristics of DOM. By combining optical characterization with the biodegradation  
109 of *Prochlorococcus*-derived DOM, our study provides fundamental data to link  
110 laboratory analyses with large-scale oceanographic survey data. This work will help us  
111 understand the role of viral infection in the composition and biodegradability of  
112 phytoplankton-released DOM and improve the knowledge of the viral impact on  
113 ecology and biogeochemistry in the ocean.

## 114 **Materials and Methods**

### 115 ***Prochlorococcus* DOM collection**

116 *Prochlorococcus* MED4 and three phages with different morphologies (myovirus P-  
117 HM2, siphovirus P-HS2 and podovirus P-SSP7) used in this work are routinely  
118 maintained at The Hong Kong University of Science and Technology (Table S1). Axenic  
119 *Prochlorococcus* strain MED4 was cultivated in eight one-litre polycarbonate bottles in  
120 Port Shelter (Hong Kong) seawater-based Pro99 medium (Pro-medium, 800 mL) with  
121 50  $\mu\text{M}$   $\text{NaHPO}_4$ , 800  $\mu\text{M}$   $\text{NH}_4\text{Cl}$ , and trace metal mix (32) at 23 °C under constant cool  
122 white light (30  $\mu\text{E m}^{-2} \text{s}^{-1}$ ) (the method used for the axenicity tests for *Prochlorococcus*  
123 is shown in supplementary methods). After reaching the early-logarithmic growth  
124 phase (an abundance of ca.  $10^8$  cells  $\text{mL}^{-1}$ ), six cultures were inoculated with myovirus  
125 P-HM2, siphovirus P-HS2, and podovirus P-SSP7 (ca.  $10^9$  particles  $\text{mL}^{-1}$ ) at a ratio of

126 1:100 (volume/volume, corresponding MOI of 0.1 ). One week later, the cultures were  
127 filtered through 0.2  $\mu\text{m}$  polycarbonate membranes (47mm, Millipore, USA). All  
128 filtrates and 2 L Pro-medium were stored in precombusted (450  $^{\circ}\text{C}$  for 6 h) 450 mL  
129 Boston round amber glass bottles (CNW, Germany) at 4  $^{\circ}\text{C}$  and used within three weeks.  
130 All filtration procedures were conducted at low pressure in a clean-hand bench. Here,  
131 we define P-HS2, P-HM2, and P-SSP7 lysates as virus-derived DOM (Pro-vDOM), the  
132 filtrate of *Prochlorococcus* culture without virus addition as Pro-exudate, Pro99  
133 medium as Pro-medium and Pro-DOM as including both Pro-exudate and Pro-vDOM.

134 Before performing dark incubation experiments, the DOC, CDOM, FDOM, and  
135 amino acid of the obtained DOM (Pro-DOM and Pro-medium) were measured (see  
136 below).

#### 137 **Dark incubation experiments**

138 To examine the biodegradability of different DOMs derived from *Prochlorococcus*  
139 and the response of the oligotrophic bacterial community to these DOM, Pro-exudate  
140 and Pro-vDOM were added to and incubated with oligotrophic seawater (Figure S1).  
141 The surface water was collected from SEATS station (a well-investigated oligotrophic  
142 station) (33) at a 5 m depth in the South China Sea, using a rosette sampler with a  
143 conductivity–temperature–depth instrument, which yielded a recorded temperature  
144 of 29.5  $^{\circ}\text{C}$  and a salinity of 33.3, on 6 November, 2016. The seawater was filtered  
145 through a 0.8  $\mu\text{m}$ -pore size membrane (the filter sets were prewashed with 20 L ultra-  
146 pure Milli-Q water, and the first 10 L seawater filtrate was discarded) to eliminate  
147 predators and particles intermediately and then dispatched into twelve 10 L acid-



148 prewashed polycarbonate carboys (wrapped with foil). The filtered seawater was  
149 amended with the following DOM sources: Pro-medium, Pro-exudate, and three  
150 *Prochlorococcus* virus lysates (namely, P-HS2 lysate, P-SSP7 lysate, and P-HM2 lysate).  
151 Studies have revealed that both DOM quality and quantity influence the microbial  
152 community (34, 35). A recent study showed that DOM quantity affects the bacterial  
153 community more than quality does (36). In this study, we added a low dose of DOM  
154 (8-15  $\mu\text{M}$ ) into each microcosm to avoid “shock” from DOM addition to microbial  
155 communities and to simulate the *in situ* conditions of the oligotrophic open ocean.  
156 Each DOM treatment had two replicates. Another two carboys contained 0.8  $\mu\text{m}$ -  
157 filtered seawater sample without any treatment and were used as the controls for this  
158 experiment. During the experiment duration, samples were collected to determine the  
159 DOC concentration, CDOM, FDOM, amino acid, prokaryotic abundance, and bacterial  
160 community.

#### 161 **Dissolved organic carbon analysis**

162 Dissolved organic carbon (DOC) samples were collected at 0, 6, 18, 36, 48, and 120 h  
163 with precombusted (450  $^{\circ}\text{C}$ , 6 h) glass pipettes and stored in precombusted (450  $^{\circ}\text{C}$ , 6  
164 h) 40 mL amber vials at -20  $^{\circ}\text{C}$  until further analysis. Three subsamples were collected  
165 from each replicate. In this study, the incubation used 0.8  $\mu\text{m}$ -filtered seawater, and  
166 the total organic carbon concentration was equivalent to the DOC concentration.  
167 Before analysis, the samples were thawed at room temperature and then acidified to  
168 pH < 2. The DOC concentration was measured using the high-temperature combustion  
169 method on a Shimadzu TOC-VCPH organic carbon analyser. Three to five injections of

170 150  $\mu\text{L}$  were performed per sample until the coefficient of variation on the analysis of  
171 replicate measurements was approximately 2%. The concentrations were determined  
172 by subtracting the values from a blank of ultra-pure Milli-Q water and dividing the  
173 result by the slope of a daily standard curve made from potassium hydrogen phthalate.  
174 All samples were checked against deep-sea reference water and low-carbon water  
175 (provided by the Hansell Organic Biogeochemistry Laboratory, University of Miami,  
176 USA). The analytical precision was  $\pm 1.7 \mu\text{mol-C L}^{-1}$  as indicated by the standard  
177 deviation of DOC measurement of deep-sea reference water (n=18).

#### 178 **Total amino acid analysis**

179 Samples for total dissolved amino acid (TDAA) analysis were directly collected  
180 from the carboys with precombusted (450 °C, 6 h) glass pipettes and stored in 40 mL  
181 precombusted (450 °C, 6 h) amber glass vials at -20 °C until analysis. The measurement  
182 of TDAA used a previously established method (37), and the detailed method and  
183 settings referred to Li and colleagues (38). Thirteen amino acids, namely, aspartic acid  
184 (Asp), glutamic acid (Glu), serine (Ser), arginine (Arg), glycine (Gly), threonine (Thr),  
185 alanine (Ala), tyrosine (Tyr), valine (Val), phenylalanine (Phe), isoleucine (Ile), leucine  
186 (Leu), and  $\gamma$ -aminobutyric acid (GABA) were measured.

187 A 2 mL sub-sample was added to a screw-top tube spiked with 2 mL concentrated  
188 HCl (trace metal grade; Fisher, USA) and sealed under nitrogen before being hydrolyzed  
189 at 110 °C for 24 h. The hydrolysed samples were dried with ultra-pure nitrogen gas,  
190 dissolved in ultra-pure Milli-Q water, and finally spiked with amino adipic acid. Then, 1  
191 mL of the obtained sample was transferred to a 2-mL vial and then reacted with 100

192  $\mu\text{L}$  of o-phthalaldehyde (OPA) solution at room temperature for 2 min. A 20  $\mu\text{L}$   
193 aliquot was injected into an HPLC system coupled with a fluorescence detector  
194 (Shimadzu RF-20A) with excitation and emission wavelengths of 330 nm and 418 nm,  
195 respectively. The separation of amino acids was accomplished using a reverse-phase  
196 C18 column (Inert Sustain, 250 $\times$ 4.6 mm, particle size 5  $\mu\text{m}$ ) at a flow rate of 1.0 mL  
197  $\text{min}^{-1}$ . Mobile phase A consisted of 0.04 M potassium phosphate monobasic buffer  
198 with 1% tetrahydrofuran, and the pH was adjusted to 6.2 with potassium hydroxide.  
199 Mobile phase B consisted of HPLC-grade methanol, acetonitrile and ultra-pure water  
200 mixed at a volume ratio of 4.5:4.5:1. The elution gradient (38) was performed over 73  
201 min. The relative standard deviation of triplicate analyses was < 3%. Ultra-pure Milli-Q  
202 water was used as the blank for every measurement batch. The mean peak areas of  
203 each amino acid in the blanks were subtracted from the corresponding peaks of all  
204 samples. The blanks were generally less than 2% of the sample signals measured in  
205 this research.

#### 206 **CDOM absorption, EEM measurement and PARAFAC modelling**

207 CDOM and FDOM sampling were performed at 0, 18, 36, 48, 72, 96, and 120 h.  
208 All CDOM and FDOM samples were kept frozen (-20  $^{\circ}\text{C}$ ) until further analysis. Storing  
209 CDOM samples at -20  $^{\circ}\text{C}$  is a commonly used method for CDOM analyses, and a  
210 number of marine DOM studies show the minimal effects from freezing/thawing on  
211 DOM optical properties (39, 40). Ultra-pure Milli-Q water was used as the absorbance  
212 and fluorescence blank. DOM absorption was measured as previously described (41).  
213 Namely, the absorption scans ranged from 240 to 800 nm at 1 nm intervals using a

214 2300 UV-Visible spectrophotometer (Techcomp, China) with a 10 cm-path length  
215 quartz cell at constant room temperature. Ultra-pure water was measured every 3  
216 samples to detect and adjust for possible instrument drift. After subtracting the  
217 average absorption value between 700 nm and 750 nm, absorbance values were  
218 converted to Napierian absorbance coefficients using the following equation:

$$219 \quad a = 2.303A/L$$

220 where  $a$  is the Napierian absorption coefficient ( $\text{m}^{-1}$ ),  $A$  is the absorbance measured  
221 by the spectrophotometer, and  $L$  is the path length (m). The spectral slope over the  
222 wavelength range from 275 to 295 nm ( $S_{275-295}$ ) was calculated by linear regression of  
223 natural log-transformed absorption spectra (42). Helms and colleagues (42)  
224 demonstrated that the  $S_{275-295}$  can be related to the relative molecular weight of DOM,  
225 and high  $S_{275-295}$  values typically indicate LMW DOM.

226 Fluorescence measurements were analysed as previously described (41). Briefly,  
227 EEMs were obtained using a Cary Eclipse (Varian, Australia) fluorimeter equipped with  
228 a 150 W Xe arc lamp. The configuration included excitation from 250 to 450 nm in 5  
229 nm intervals with acquisition from 280 to 600 nm at 2 nm intervals and 10 nm and 5  
230 nm slit widths on the excitation and emission modes, respectively. The scan speed was  
231  $1920 \text{ nm min}^{-1}$ , with the photomultiplier voltage set to 800 V. The EEMs of the samples  
232 were blank corrected and Raman-normalized using ultra-pure Milli-Q water EEMs  
233 scanned on the same day. In total, 168 EEM spectra were modelled using parallel factor  
234 analysis (PARAFAC) with MATLAB 7.5 and the DOMFluor toolbox (43). Split-half  
235 validation was used to determine the number of fluorescent components. The

236 fluorescence intensity of each fluorescent component was evaluated using the  
237 maximum fluorescence. EEM maps of *Prochlorococcus*-derived DOM were obtained  
238 after subtracting the blank and normalizing to the ultra-pure Milli-Q water Raman peak  
239 scanned on the same day. The fluorescent components of the obtained  
240 *Prochlorococcus*-derived DOM stocks were obtained by the traditional “peak-picking”  
241 method (44).

#### 242 **Prokaryotic abundance analysis**

243 The prokaryotic abundance was determined at 0, 6, 12, 18, 24, 36, 48, 72, 96 and  
244 120 h with the established methods (45). At each sampling time, 1.8 mL subsamples  
245 were fixed with a final concentration of 0.5% glutaraldehyde for 15 min in the dark,  
246 flash-frozen in liquid nitrogen and stored at -80 °C until analysis. Before analysis, the  
247 frozen prokaryotic abundance samples were thawed in a 37 °C bath. Then, 990 µL  
248 samples were stained with 10 µL SYBR Green I (Sigma-Aldrich, St. Louis, MO) for 15  
249 min in the dark, and 10 µL 1 µm calibration beads (BD Bioscience) were added as  
250 reference before counting by flow cytometer (BD Accuri C6, USA), and prokaryotes  
251 were identified in plots of red fluorescence vs. green fluorescence. Autotrophic  
252 picoplankton abundance were analysed on a BD FACSAria flow cytometer, and 1 µm  
253 calibration beads were used for the flow rate calibration; autotrophic picoplankton are  
254 identified in plots of side scatter vs. red fluorescence. Heterotrophic bacterial  
255 abundance were obtained by subtracting autotrophic cell abundance from prokaryotic  
256 abundance. The flow cytometric data were analysed with the BD Accuri C6 software  
257 and FCS Express software.

258 **DNA extraction, sequencing and analysis**

259 One litre of seawater from each treatment was collected at 0, 18, 36, 48, and 120  
260 h and filtered through 0.2 µm polycarbonate filters (Millipore, 47 mm diameter) under  
261 low pressure (less than 30 kPa), and the filters were stored at -80 °C until further  
262 analysis. Note that samples at 0 h were collected from only the control, and all the  
263 treatments shared the initial bacterial community structure of these samples. DNA  
264 was extracted from the samples using a previously described method (46).

265 The 16S rRNA gene V3-V4 region was amplified using a specific primer pair (341F-  
266 806R) (47) with a barcode. All PCRs were carried out with Phusion® High-Fidelity PCR  
267 Master Mix (New England Biolabs). Samples with bright main bands between 450 and  
268 550 bp were chosen, and the band contents were purified with the Qiagen Gel  
269 Extraction Kit (Qiagen, Germany). The amplicons were paired-end sequenced using the  
270 HiSeq2500 platform (Illumina, Inc., San Diego, CA, USA). Sequences were assigned to  
271 each sample based on the barcode and truncated by cutting off the barcode and  
272 primer sequence. Sequence assembly was conducted with FLASH (V1.2.7)(48), and  
273 low-quality sequences were filtered under specific filtering conditions according to the  
274 QIIME (V1.7.0) quality control process (49). Chimeric sequences were detected with  
275 the Genomes Online Database (GOLD) using the UCHIME algorithm and then removed  
276 (50). Then, effective tags were finally obtained.

277 Sequence analysis was performed by UPARSE software (UPARSE v7.0.1001) (51).  
278 Sequences were assigned to the same OTUs at 97% similarity, and a representative  
279 sequence for each OTU was screened for further annotation. The OTU taxonomic

280 information was annotated using the RDP classifier (Version 2.2) (52) with the  
281 Greengenes database (53). The OTU abundance was normalized using a standard  
282 sequence number corresponding to the sample containing the fewest sequences.  
283 Subsequent analyses of alpha diversity and beta diversity were performed based on  
284 this output normalized data.

### 285 **Microbial network analysis**

286 A network was constructed following a previously published method (54), with some  
287 modification. OTUs were defined at 97% similarity, and those with a relative  
288 abundance above 0.1% in one sample that appeared in more than two samples of all  
289 treatments were selected. We calculated all possible Spearman's rank correlations  
290 between these OTUs. We considered a valid co-occurrence event to be a robust  
291 correlation if the Spearman's correlation coefficient was  $> 0.6$  and a statistically  
292 significant  $P$ -value  $< 0.01$  was present. The networks of each treatment were displayed  
293 separately with Gephi 0.9.2. To describe the topology of the network, some basic  
294 indices (node, edge, average degree, graph density, and others) were calculated.

### 295 **Statistical analysis**

296 Statistical analyses, including t-tests to examine the differences in the optical  
297 parameters of the generated DOM between Pro-exudate and Pro-vDOM, one-way  
298 ANOVAs to compare the differences in the heterotrophic bacterial abundance and  
299 DOM utilization rate, the calculation of the specific growth rate ( $\mu$ ) according to the  
300 general linear regression slope between the log-transformed bacterial abundance and  
301 growth time and univariate analysis to test the differences between the resulting  $\mu$

302 values, were performed using IBM SPSS Statistics 25.0 (IBM Corp., USA).

303 Nonmetric multidimensional scaling (NMDS) analysis for the bacterial community  
304 structure and the SIMPROF test for bacterial community similarity were performed  
305 with Primer 6 (PRIMER-E, UK). Bacterial relative abundance data were not transformed  
306 during NMDS and SIMPROF analysis. The R package (version 3.4.3) was used for the  
307 redundancy analysis (RDA analysis). Before RDA analysis, bacterial relative abundance  
308 data were transformed by Hellinger transformation, environmental factor (DOC,  $S_{275-}$   
309  $_{295}$ ,  $a_{280}$ ,  $a_{254}$ , C1, C2, C3, C4, and C5) data were zero-centred and normalized, and  
310 covariability among environmental factors were examined using variance inflation  
311 factors (factors that least than 10 were selected). RDA analysis was conducted with  
312 vegan package via permutation test (999 permutations).

### 313 **Data availability**

314 The sequences reported in this paper have been deposited to the National Center  
315 for Biotechnology Information database under BioProject no. PRJNA644149 (releasing  
316 at November 7, 2020).

## 317 **Results**

### 318 **DOM derived from *Prochlorococcus***

319 DOC concentrations of Pro-exudate and Pro-vDOM were much higher than that  
320 of Pro-medium (Table 1). The optical properties of DOM derived from *Prochlorococcus*  
321 were investigated using a UV-visible spectrophotometer and a spectrofluorometer. As  
322 shown in Table 1, the ultraviolet absorbance coefficient at 254 nm ( $a_{254}$ ) of Pro-vDOM  
323 (except P-HS2 lysate) were higher than those of Pro-exudate and the magnitude of this



324 trend varied between the different phage types used. Our data showed that the  $S_{275-}$   
325  $_{295}$  values of Pro-vDOM were significantly higher than those of Pro-exudate (t-test,  
326  $P<0.05$ ). This indicated that Pro-vDOM contained more LMW DOM than did Pro-  
327 exudate.

328 Pro-exudate and three Pro-vDOM shared similar fluorescence excitation-emission  
329 matrices (EEMs) (Figure 1). According to the EEMs of Pro-DOM, *Prochlorococcus*  
330 produced both protein-like (peak T) and humic-like fluorescent materials (peak A, C,  
331 M) through exudation and viral lysis (Table 1). Both Pro-exudate and Pro-vDOM  
332 showed the most prominent peaks at 250/466 nm (ex/em), which corresponded to  
333 previously defined “terrestrial humic-like” substances (peak A) (44). The fluorescence  
334 intensity of the peak at 335/404 nm (ex/em), which corresponds to marine humic-like  
335 materials (peak M) (44), was the second highest. Another humic-like peak assigned to  
336 peak C (ex/em 355/450 nm) appeared in all Pro-DOM. Compared to the peaks  
337 observed for Pro-medium, peak M and peak C were the most increased components.  
338 The fluorescence intensity of peak M of Pro-vDOM was significantly higher than that  
339 of Pro-exudate (t-test,  $P<0.05$ ). In the protein-like region, one peak at ex/em 275/340  
340 nm (peak T) was found in Pro-exudate and Pro-vDOM. Podovirus P-SSP7-mediated Pro-  
341 vDOM showed the highest fluorescence intensity for protein-like peak T.

342 The total dissolved amino acid (TDAA) analysis showed that Asp, Glu, Ala and Gly  
343 were the dominant amino acids in Pro-DOM (Table S2). Compared with those of Pro-  
344 medium, the DOC-normalized TDAA of Pro-DOM were significantly elevated, and the  
345 TDAA concentrations of the P-HS2 and P-SSP7 lysates were higher than those of Pro-

346 exudate, supporting the above shown  $S_{275-295}$  results (Table 1). In addition, the total  
347 concentration of the 14 amino acids of Pro-vDOM increased differently than did that  
348 of Pro-exudate (Table S2). Together, our data showed that both the quantity and  
349 quality of DOM were different between Pro-exudate and Pro-vDOM.

### 350 **Microbial utilization of DOM**

351 After DOM addition, the initial DOC concentration of all treatments ranged from  
352 80.4 (Pro-medium treatment) to 89.4  $\mu\text{M}$  (P-HS2 lysate treatment), corresponding to  
353 DOC increases of 7.9% to 20.0% from the DOC concentration in the control (74.4  $\mu\text{M}$ )  
354 (Table S3). During the 120 h incubation experiment, the DOC concentration of the  
355 control remained stable, while those of the DOM addition treatments rapidly  
356 degraded in the first 18 h (Figure 2a). The amount of consumed DOC ranged from 3.6  
357  $\mu\text{M}$  to 8.6  $\mu\text{M}$  in the first 18 h, corresponding to 4.5% to 9.6% of the initial DOC content  
358 (Table S3). The DOC consumption ratio of Pro-vDOM was higher than that of Pro-  
359 exudate at 18 h and 120 h.

360 Figure 2b displays the CDOM spectral slope  $S_{275-295}$  of each treatment at a specific  
361 sampling time during the incubation period. After DOM addition, the initial spectral  
362 slopes ranked as follows: control > Pro-vDOM > Pro-exudate > Pro-medium. This result  
363 suggested that the Pro-exudate treatment contained much more high-molecular-  
364 weight DOM than did the Pro-vDOM treatments at the beginning of incubation. At the  
365 end of the incubation, all DOM addition treatments had similar spectral slopes,  
366 however, these slopes differed from those at the beginning (Figure 2b), hence resulting  
367 in the spectral slope of Pro-vDOM decreasing more compared to that of Pro-exudate.

368 Five fluorescent components were identified using parallel factor analysis  
369 (PARAFAC), including two protein-like and three humic-like components (Figure 3, left  
370 panel). Components 1 and 5 (C1 and C5) were characterized as amino acid-like DOM  
371 (44) and displayed relatively narrower emission spectra with maxima below 350 nm.  
372 C1 displayed excitation maximum at 275 nm and one emission maximum at 332 nm,  
373 which was similar to tryptophan-like peak T. C5 had an excitation/emission maximum  
374 at 275/300 nm, similar to tyrosine-like peak B. Components 2, 3 and 4 (C2, C3 and C4)  
375 were assigned to humic-like FDOM. C2 exhibited two peaks with excitation maxima at  
376 255/365 nm and emission at 456 nm and was categorized as a combination of  
377 terrigenous humic-like peaks A and C (44). C3 exhibited excitation maxima at <250 nm  
378 with 368 nm emission. This matched with the C4 reported by Yamashita and colleagues  
379 (55), and C4 is thought to be a microbe-derived humic-like component. The peak of C4  
380 at 325/396 nm (ex/em) corresponded to marine humic-like fluorescence (peak M) (56).

381 Compared with that of the control, the initial fluorescence intensities of the  
382 DOM-addition treatments increased to different degrees, and the most enriched of  
383 the five components was C1 (Figure S2), indicating that the DOM quality of all  
384 treatments changed after DOM addition. Since C5 contributes only a small part (10-  
385 20%) of the protein-like fluorescence intensity, tryptophan-like C1 was selected as  
386 representative of the protein-like components for subsequent analysis. The  
387 fluorescence intensity of C1 sharply decreased over the entire incubation period in the  
388 treatments but not in the control. After 120 h incubation, most (50-70%) C1 was  
389 degraded in the Pro-medium and Pro-DOM treatments. Peaks A and C (referred to as

390 C2 in the incubation experiment) showed higher fluorescence intensities for Pro-DOM  
391 than for Pro-medium (Table 1), and the intensity of C2 had different increases from 24  
392 or 36 h of incubation for different DOM treatments (Figure 3). These results suggest  
393 that C2 is produced not only by *Prochlorococcus* but also by heterotrophic bacteria  
394 under specific conditions. Moreover, C4 of the Pro-DOM treatment presented a higher  
395 fluorescence intensity than did that of the Pro-medium treatment and showed an  
396 intensity increase of 30-50%, though C4 represented only a small proportion of FDOM.

### 397 **Growth of heterotrophic bacteria**

398 During the course of the experiment, the heterotrophic bacterial abundances  
399 increased during the first phase, and later, this increase slowed and reached a  
400 stationary phase in all five treatments (Figure 4). In the control, the bacterial  
401 abundance increased from  $3.5 \times 10^5$  cells  $\text{mL}^{-1}$  at 0 h to  $8.4 \times 10^5$  cells  $\text{mL}^{-1}$  at 120 h. The  
402 bacterial abundances of the five treatments increased from an average of  $3.1 \times 10^5$  cells  
403  $\text{mL}^{-1}$  at the beginning to between  $12 \times 10^5$  cells  $\text{mL}^{-1}$  and  $15 \times 10^5$  cells  $\text{mL}^{-1}$  at the end,  
404 with a tendency of Pro-vDOM treatments showing higher bacterial abundances  
405 compared to the Pro-exudate treatment.

406 During the incubation, the growth curves of all treatments showed log growth  
407 and a stationary phase. The bacterial specific growth ( $\mu$ ) of the log-growth phase was  
408 estimated by the regression slope of the natural log-transformed bacterial abundance.  
409 The  $\mu$  values of the Pro-DOM and Pro-medium treatments were significantly higher  
410 than that of the control (univariate analysis of variance,  $p < 0.001$ ), and the  $\mu$  values of  
411 the P-HS2 and P-SSP7 lysate treatments were significantly higher than that of the Pro-

412 exudate treatment (univariate analysis of variance,  $p = 0.007$  and  $0.016$ , respectively)  
413 (Table S4). Although there was no significant difference,  $\mu$  of the P-HM2 lysate  
414 treatment ( $0.91 \text{ d}^{-1}$ ) was also higher than that of the Pro-exudate treatment ( $0.83 \text{ d}^{-1}$ )  
415 (Table S4). After the stationary growth phase was reached, the bacterial abundance of  
416 all Pro-vDOM treatments were significantly higher than that of the Pro-exudate  
417 treatment (one-way ANOVA,  $P < 0.05$ ) (Table S5). Therefore, Pro-vDOM showed higher  
418 bioavailability compared to Pro-exudate.

### 419 **Bacterial diversity and community composition**

420 During the incubation period, the alpha diversity (Shannon and Simpson indices)  
421 of the bacterial community in the control and Pro-medium treatments remained  
422 relatively constant, whereas those of the Pro-DOM treatments decreased sharply  
423 during the first 48 h and then remained constant (Figure S3). It was also found that the  
424 alpha diversity of Pro-vDOM was lower than that of Pro-exudate.

425 Alteromonadales, Rhodospirillales and SAR11 accounted for more than 50% of  
426 the bacterial community throughout the experiment. The initial primary groups were  
427 *Prochlorococcus* and *Pelagibacter*, and they shifted to *Nautella*, *Alteromonas*,  
428 *Prochlorococcus*, and *Pelagibacter* at the end of the experiment in the control; to  
429 *Alteromonas*, *Pelagibacter*, and *Thiomicrospira* in the Pro-medium samples; and to  
430 *Nautella* and *Alteromonas* in the Pro-DOM samples (Figure 5). During the incubation,  
431 the relative abundances of Rhodobacterales and Alteromonadales increased, while  
432 those of the SAR11 clade and cyanobacteria decreased in all treatments. *Nautella* and  
433 *Alteromonas* were the two groups that responded quickly to Pro-DOM addition and

434 predominated in the late period of the experiment in all DOM-amended treatments.

435 As shown in Figure 6, distinct changes in the bacterial community structure  
436 mainly happened within 36 h, and then the bacterial community structure remained  
437 stable. During the experimental period, the bacterial structure of the control had a  
438 relatively small change compared with those of samples receiving DOM addition.  
439 Compared with that of the Pro-medium treatment, the bacterial community structures  
440 of Pro-DOM treatments had a distinct succession trajectory. A difference also existed  
441 between the structures of Pro-exudate and Pro-vDOM treatments (especially for the  
442 P-HS2 and P-SSP7 lysates). From 36 h, the similarity of the bacterial community  
443 structure of the Pro-vDOM treatments were significantly different from that of the Pro-  
444 exudate treatment at the corresponding sampling time (SIMPROF test,  $p = 0.001$ ), and  
445 the bacterial communities of the P-HS2 lysate and P-SSP7 lysate treatments were  
446 similar (84.6%) but significantly different from that of the Pro-exudate treatment at  
447 the 36 h and 48 h sampling points (SIMPROF test,  $p = 0.001$ ). This indicated that the  
448 Pro-exudate and Pro-vDOM treatments have different effects on microbial community  
449 succession.

450 OTU-based microbial co-occurrence network analysis showed that most of the  
451 highly connected OTUs were assigned to Alpha- and Gammaproteobacteria (Figure 7),  
452 indicating that bacterial species in these two classes were key components of the  
453 microbial community. DOM addition significantly increased the positive interactions  
454 among microorganisms, and the graph density of the network of Pro-DOM treatments  
455 was more than two times higher than that of the control and Pro-medium treatment

456 (Table S6). The increased interactions were mainly due to some specific OTUs that  
457 belonged to Alphaproteobacteria in the Pro-medium and Pro-exudate treatments and  
458 to Alphaproteobacteria, Gammaproteobacteria and cyanobacteria in the Pro-vDOM  
459 treatments. The highly connected OTUs also differed among these DOM treatments.  
460 In the Pro-medium treatment, the OTUs belonged to the SAR11 clade and  
461 *Prochlorococcus. Rhodospirillaceae* and the SAR11 clade (except in the P-HM2 lysate  
462 treatment) dominated in all Pro-DOM treatments, and *Prochlorococcus* also appeared  
463 to have a close interaction with other OTUs in the Pro-vDOM treatments (except in the  
464 P-HM2 lysate treatment). The negative interactions among microorganisms were also  
465 affected by DOM addition (Table S6). There were small changes in the negative  
466 interaction in the Pro-medium and Pro-exudate treatments compared with the control.  
467 Compared with the Pro-exudate treatment, Pro-vDOM treatments had an apparent  
468 increase in negative edges and nodes with negative interactions with other nodes.

## 469 Discussion

### 470 Viral lysis alters the quality of DOM released by *Prochlorococcus*

471 In this work, our DOC, CDOM, FDOM and amino acids data showed that viral lysis  
472 altered the production and composition of DOM released by *Prochlorococcus*, which  
473 is the most important photosynthetic picophytoplankton in the oligotrophic ocean.  
474 This finding is consistent with those of previous studies based on other phytoplankton.  
475 Viral infection alters the lipid composition of *Emiliana huxleyi* cellular materials (9)  
476 and the composition of DOM released by *Micromonas pusilla* and *Synechococcus* (4,  
477 13, 14). Treatments with Pro-vDOM, which contained intracellular materials of hosts,

478 resulted in a higher  $a_{254}$ , amino acid concentration and spectral slope  $S_{275-295}$  compared  
479 to treatment with Pro-exudate. During the incubation, Pro-vDOM treatments resulted  
480 in a higher DOC degradation rate than the Pro-exudate treatment, and their  $S_{275-295}$   
481 values decreased more than that of the Pro-exudate treatment did (Table S3 and Figure  
482 2b). Microbial degradation induces the decrease of  $S_{275-295}$  as a result of LMW DOM  
483 consumption (42). These results suggested that more labile LMW DOM was released  
484 and then consumed in the Pro-vDOM treatments than in the Pro-exudate treatment.  
485 In addition, the TDAA carbon yield, which indicates the degree of bioavailability of  
486 DOM (57), of the Pro-vDOM treatments were much higher than that of the Pro-  
487 exudate treatment at the beginning and close (0.8-1.1%) at the end of incubation  
488 (Figure S4), resulting in the TDAA carbon yield of Pro-vDOM treatments decreasing  
489 more than that of the Pro-exudate treatment. This indicated that Pro-vDOM has higher  
490 bioavailability than Pro-exudate. This result was further supported by the finding that  
491 the heterotrophic bacterial growth rate and abundance of the Pro-vDOM treatments  
492 were significantly higher than those of the Pro-exudate treatment (Table S4, S5),  
493 suggesting that Pro-vDOM was easier to convert to biomass than the Pro-exudate. It  
494 is also possible that the labile DOM released by viral lysis may enhance the accessibility  
495 of RDOM to bacterial remineralization due to the priming effect (58). Therefore, the  
496 viral lysis of *Prochlorococcus* might fuel heterotrophic bacterial activity and,  
497 subsequently, the microbial loop in vast oligotrophic oceans. In the initial viral shunt  
498 concept (59), it was predicted that heterotrophic bacterial production is stimulated by  
499 viral lysis products, i.e., by organic matter that enters the DOM pool and is hence not



500 transferred to higher trophic levels by grazing (5). Here, we present an additional  
501 interpretation, i.e., that viral lysis not only increases the concentration of the DOM  
502 pool, but also changes the quality of the DOM towards higher bioavailability.

### 503 **Bacterial community fuelled by different sources of DOM**

504 NMDS analysis showed that Pro-DOM had significant effects on the microbial  
505 community succession trajectories (Figure 6). Compared with the Pro-medium  
506 treatment, the Pro-DOM treatments had distinct community structures during the  
507 entire incubation period, suggesting that Pro-DOM had a significant role in shaping the  
508 microbial community. This is consistent with previously observed pronounced effects  
509 of phytoplankton-derived DOM (such as from diatoms and *Synechococcus*) on the  
510 bacterial community (60, 61). Importantly, we observed that the microbial community  
511 of the Pro-vDOM treatments had different succession trajectories compared with that  
512 of the Pro-exudate treatment (20). Previous works have suggested that the microbial  
513 community structure might be affected by both DOM quality and quantity (34-36). Our  
514 redundancy analysis (RDA) showed that the DOM composition could explain 50% of  
515 the total variation in the bacterial community composition, while the DOC  
516 concentration had a minor effect. This result was contrary to that reported by  
517 Sarmiento and colleagues (36), who found that DOM quantity affects bacterial  
518 communities more than quality. A possible reason for this difference might be the  
519 relatively larger DOC concentration range (10, 30 and 100  $\mu\text{M}$ ) in their experiment than  
520 in our experiments. For example, high DOC concentrations could shift the bacterial  
521 community towards faster-growing OTUs (62). Therefore, the different responses of

522 the microbial community structure to Pro-vDOM and Pro-exudate treatments could  
523 reflect differences in DOM quality due to providing specific ecological niches for  
524 bacteria since similar initial DOC concentration were used in this study.

525 In addition, our work showed that vDOM produced by morphologically different  
526 phages probably have diverging ecological roles, since they affected the bacterial  
527 growth rate (Figure 4) and bacterial diversity (Figure S3) in different ways. These  
528 differences may be related to DOM quality changes (such as the amino acid  
529 composition and concentration and protein-like FDOM production) due to variations  
530 in host-phage interactions. Thompson and colleagues demonstrated that marine  
531 cyanophages carried and expressed auxiliary metabolic genes (AMGs) and may have  
532 redirected the host carbon metabolism (63). It was reported that the three  
533 cyanophages had different burst sizes and AMGs (64), which may lead to differences  
534 in the quality of the organic matter in Pro-vDOM.

535 Furthermore, RDA analysis illustrated that specific microbial taxa were linked to  
536 DOM characteristics (Figure 8). The absorption coefficient  $a_{280}$  and protein-like FDOM  
537 C1 and C5 were positively correlated with the relative abundance of Alteromonadales,  
538 which was one of the dominant groups in the incubation. These results are probably  
539 explained by the fact that Alteromonadales was mainly responsible for CDOM removal  
540 in the dark incubation. For C4, the humic-like FDOM component was positively related  
541 to Rhodobacterales, indicating that Rhodobacterales might be the major biological  
542 factor affecting the fate of humic-like DOM in dark conditions. Though both  
543 Alteromonadales and Rhodobacterales were the dominant groups in this experiment,

544 the major roles of the two maybe differ in carbon processing. Alteromonadales have a  
545 broad substrate preference relative to that of Rhodobacterales (65-67) and may apply  
546 diverse complementary growth strategies to rapidly respond to external disturbances.  
547 The coefficients  $a_{280}$ , C1, and C5 closely correlated with early samples (in 18 h), and  
548 C4 was correlated with later samples. This indicates that the early period was the DOM  
549 removal and biomass accumulation phase and that the late phase was responsible for  
550 humic-like DOM accumulation. This is supported by previous works showing that  
551 bacteria incorporate labile DOM into biomass but respire low-quality DOM and  
552 produce humic-like by-products (68, 69).

553 In microbial co-occurrence network analysis, positive relationships indicate co-  
554 operation, co-colonization or niche overlap while negative relationships suggest  
555 competition or prey-predator relationship (70). Compared with the control and Pro-  
556 medium treatment, Pro-DOM addition significantly increased the positive relationship  
557 among microorganisms (Table S6). The possible reason was that Pro-DOM is a complex  
558 DOM mixture and needs additional microbial co-operation to be utilized. Furthermore,  
559 the average degree of the network of Pro-vDOM was higher than that of Pro-exudate  
560 (Table S6), indicating that denser interactions among species appeared in the Pro-  
561 vDOM treatments than in the Pro-exudate treatment. In addition, negative  
562 interactions increased in the Pro-vDOM treatments but not in the Pro-exudate  
563 treatment. Detailed analysis showed that the negative interactions mainly happened  
564 between the high-relative abundance OTUs (*Nautella*, *Alteromonas*, *Marinomonas*)  
565 and other OTUs. These results suggested that these bacteria may have a greater

566 competitive pressure in Pro-vDOM treatments than in the Pro-exudate treatment,  
567 indicating that Pro-vDOM is likely more labile to oligotrophic microorganisms  
568 compared to Pro-exudate.

569 **Implication: the impact of viral lysis on the production and**  
570 **transformation of DOM in the ocean**

571 Peak M represents the primary humic-like material in *Prochlorococcus*-derived FDOM  
572 (Table 1), which is thought to be autochthonous humic-like DOM in the global ocean  
573 with a ubiquitously distributed microbial origin (44). The relatively high peak-M  
574 fluorescence intensity of the Pro-vDOM treatments indicated that viral lysis is a  
575 pathway that considerably contributes to the release of humic-like materials produced  
576 by *Prochlorococcus*. Previous global and regional surveys show that chlorophyll *a* is  
577 closely related to the distribution of peak M in oligotrophic epipelagic oceans (30, 71),  
578 where *Prochlorococcus* is the numerically dominant phytoplankton (22). In addition,  
579 *Prochlorococcus* has a similar vertical distribution pattern to that of peak M in the open  
580 ocean (30, 72). This indicates that viral lysis of *Prochlorococcus* is an important humic-  
581 like DOM source in the ocean. Considering the wide distribution and long turnover  
582 times (610 years) of peak M in the ocean (73), viral lysis of *Prochlorococcus* contributes  
583 to the recalcitrant DOM pool in the water column through microbial carbon pump (17).

584 Our study with isolates demonstrates that viral lysis is a source of labile and  
585 humic-like substances. It has been reported that cyanophage infection redirects host  
586 metabolism (63, 74), and it has been proposed that phage-encoded AMGs are  
587 responsible for this reprogramming (75). This suggests that viral infection plays a vital

588 role in affecting the host metabolism and the quality of host-released DOM and could  
589 have contributed to our findings. Moreover, virus-induced mortality contributes  
590 significantly to marine phytoplankton losses (5, 7). Therefore, we hypothesize that viral  
591 lysis is also a potentially important source of labile and humic-like material in the global  
592 ocean (4, 16).

### 593 **Methodological limitations**

594 Microcosm incubation is one of the approaches widely used to assess the  
595 availability of DOM for natural microorganisms (12, 36, 76). In our experimental setup,  
596 to eliminate grazing in the incubation, 0.8- $\mu\text{m}$  filtration is used to remove predators  
597 such as heterotrophic nanoflagellates and particles (12, 60, 77). Previous studies  
598 showed that 1  $\mu\text{m}$  or 0.8  $\mu\text{m}$  filtration can eliminate all heterotrophic nanoflagellates  
599 in most coastal and open regions of the South China Sea and the Atlantic Ocean (78,  
600 79). However, the filtration inevitably results in a certain loss of bacterial cells and the  
601 alteration of bacterial growth. To minimize these effects as much as possible, we used  
602 a low filtration pressure and polycarbonate membranes instead of glass fiber  
603 membranes, which can reduce the effect of filtration on the selective loss of bacteria  
604 (80).

605 During *Prochlorococcus* DOM preparation, we used a standard culture medium,  
606 Pro99 (32), to culture *Prochlorococcus* under continuous-light conditions for a better  
607 cell yields. It is worth pointing out that the nutrients concentrations (N/P) of Pro99  
608 medium were higher than those in natural sea water (32 and references therein). So  
609 far, there is no evidence indicating that the physiological and ecological characteristics

610 of *Prochlorococcus* grown in Pro99 are different from those *in situ*. For example, their  
611 temperature optima and light requirements are consistent with their distribution in  
612 the ocean (72). However, it is unknown whether the modification of these culture  
613 conditions affect the *Prochlorococcus* DOM composition released during viral infection.  
614 In addition, in accordance with previous studies (60, 65, 76), the present study added  
615 a relatively lower percentage of DOC into the incubation systems compared with  
616 environmental conditions. However, the DOM amendments should be higher than the  
617 amount of DOC released by *Prochlorococcus* in *in situ* environments. Based on the  
618 available data regarding *Prochlorococcus* viral mortality rate (8, 24, 25), cellular carbon  
619 content (81) and DOC exuded rate (3), it is estimated that *Prochlorococcus* contributed  
620 DOC of less than  $1 \mu\text{mol-C L}^{-1} \text{d}^{-1}$  under *in situ* conditions. Therefore, the addition of  
621 DOM may impact and will probably stimulate, bacterial growth. The possible  
622 differences in the quantity and quality of the *Prochlorococcus* DOM between our  
623 microcosm and natural environments need to be considered when applying our  
624 conclusions to biogeochemical studies. Moreover, viral lysis contributes to the  
625 production of both dissolved and particulate (cell debris) organic matter. Most studies,  
626 including the present one, have focused on DOM (12, 16, 21). To obtain a complete  
627 view of viral-driven production and transformation of organic matter, more  
628 investigations on organic particles generated during lysis are needed.

## 629 **Conclusion**

630 In summary, we demonstrated that viral lysis altered the quality and quantity of  
631 DOM released by *Prochlorococcus*, and hence, viral lysates of *Prochlorococcus* might

632 be a pathway that considerably contributes to marine CDOM and humic-like DOM  
633 pools. These results are an important step towards linking laboratory studies and large-  
634 scale oceanographic surveys by potentially allowing to identify sources of vDOM in the  
635 ocean. *Prochlorococcus* lysates were more labile compared to the *Prochlorococcus*  
636 exudate and shaped the microbial community with different succession trajectories.  
637 Under the conditions of global climate change, the distribution of *Prochlorococcus*  
638 might broaden, its abundance might increase (22), and the contribution of viral lysis  
639 to phytoplankton mortality might be enhanced (8). The data suggest that viral infection  
640 of *Prochlorococcus* may play an important role in shaping DOM cycling and pooling in  
641 oligotrophic oceans.

#### 642 **Acknowledgements**

643 This work was supported by the National Natural Science Foundation of China projects  
644 (41861144018 to N. J., 91951209 to R. Z., 41876083 to W. G., 41676059 and 41890801  
645 to X. L), the Research Grants Council of the Hong Kong Special Administrative Region,  
646 China (16102317) to Q. Z., and the 111 Program of Xiamen University to M.G.W. We  
647 thank the captain, crew, and scientists aboard the R/V Shiyan III, led by chief scientist  
648 Jia Sun, for their support during the cruise. Thanks to Qiaoyun Qin for assistance in  
649 using R software (RDA analysis) and Adobe Illustrator (Figure S1), Jing Xu for her  
650 technical support during FDOM data analysis, and three anonymous reviewers whose  
651 comments improved the manuscript.

#### 652 **Competing interests**

653 The authors declare no competing interests.

654 **Additional information**

655 Supplementary information is available at the Applied and Environmental  
656 Microbiology's website.

657 **References**

- 658 1. Field CB, Behrenfeld MJ, Randerson JT, Falkowski P. 1998. Primary Production of the Biosphere:  
659 Integrating Terrestrial and Oceanic Components. *Science* 281:237.
- 660 2. Falkowski PG, Raven JA. 2007. Aquatic Photosynthesis in Biogeochemical Cycles, p 364-410. *In*  
661 Falkowski PG, Raven JA (ed), Aquatic Photosynthesis, Second Edition ed. Princeton University  
662 Press.
- 663 3. Bertilsson S, Berglund O, Pullin MJ, Chisholm SW. 2005. Release of dissolved organic matter by  
664 Prochlorococcus. *Vie Et Milieu-Life and Environment* 55:225-231.
- 665 4. Lønborg C, Middelboe M, Brussaard CPD. 2013. Viral lysis of *Micromonas pusilla*: impacts on  
666 dissolved organic matter production and composition. *Biogeochemistry* 116:231-240.
- 667 5. Fuhrman JA. 1999. Marine viruses and their biogeochemical and ecological effects. *Nature*  
668 399:541-548.
- 669 6. Thornton DCO. 2014. Dissolved organic matter (DOM) release by phytoplankton in the  
670 contemporary and future ocean. *European Journal of Phycology* 49:20-46.
- 671 7. Suttle CA, Chan AM, Cottrell MT. 1990. Infection of phytoplankton by viruses and reduction of  
672 primary productivity. *Nature* 347:467.
- 673 8. Mojica KDA, Huisman J, Wilhelm SW, Brussaard CPD. 2016. Latitudinal variation in virus-  
674 induced mortality of phytoplankton across the North Atlantic Ocean. *ISME J* 10:500-513.
- 675 9. Evans C, Pond DW, Wilson WH. 2009. Changes in *Emiliana huxleyi* fatty acid profiles during  
676 infection with *E. huxleyi* virus 86: physiological and ecological implications. *Aquatic Microbial*  
677 *Ecology* 55:219-228.
- 678 10. Chrost RH, Faust MA. 1983. Organic carbon release by phytoplankton: its composition and  
679 utilization by bacterioplankton. *Journal of Plankton Research* 5:477-493.
- 680 11. Chen W, Wangersky PJ. 1996. Rates of microbial degradation of dissolved organic carbon from  
681 phytoplankton cultures. *Journal of Plankton Research* 18:1521-1533.
- 682 12. Zhao Z, Gonsior M, Schmitt-Kopplin P, Zhan Y, Zhang R, Jiao N, Chen F. 2019. Microbial  
683 transformation of virus-induced dissolved organic matter from picocyanobacteria: coupling of  
684 bacterial diversity and DOM chemodiversity. *ISME J* doi:10.1038/s41396-019-0449-1.
- 685 13. Ma XF, Coleman ML, Waldbauer JR. 2018. Distinct molecular signatures in dissolved organic  
686 matter produced by viral lysis of marine cyanobacteria. *Environmental Microbiology* 0.
- 687 14. Zhao Z, Gonsior M, Luek J, Timko S, Ianiri H, Hertkorn N, Schmitt-Kopplin P, Fang XT, Zeng QL,  
688 Jiao NZ, Chen F. 2017. Picocyanobacteria and deep-ocean fluorescent dissolved organic matter  
689 share similar optical properties. *Nature Communications* 8:15284.
- 690 15. Fiore CL, Longnecker K, Soule MCK, Kujawinski EB. 2015. Release of ecologically relevant  
691 metabolites by the cyanobacterium *Synechococcus elongatus* CCMP 1631. *Environmental*  
692 *Microbiology* 17:3949-3963.
- 693 16. Gobler CJ, Hutchins DA, Fisher NS, Cospere EM, Sanudo-Wilhelmy SA. 1997. Release and



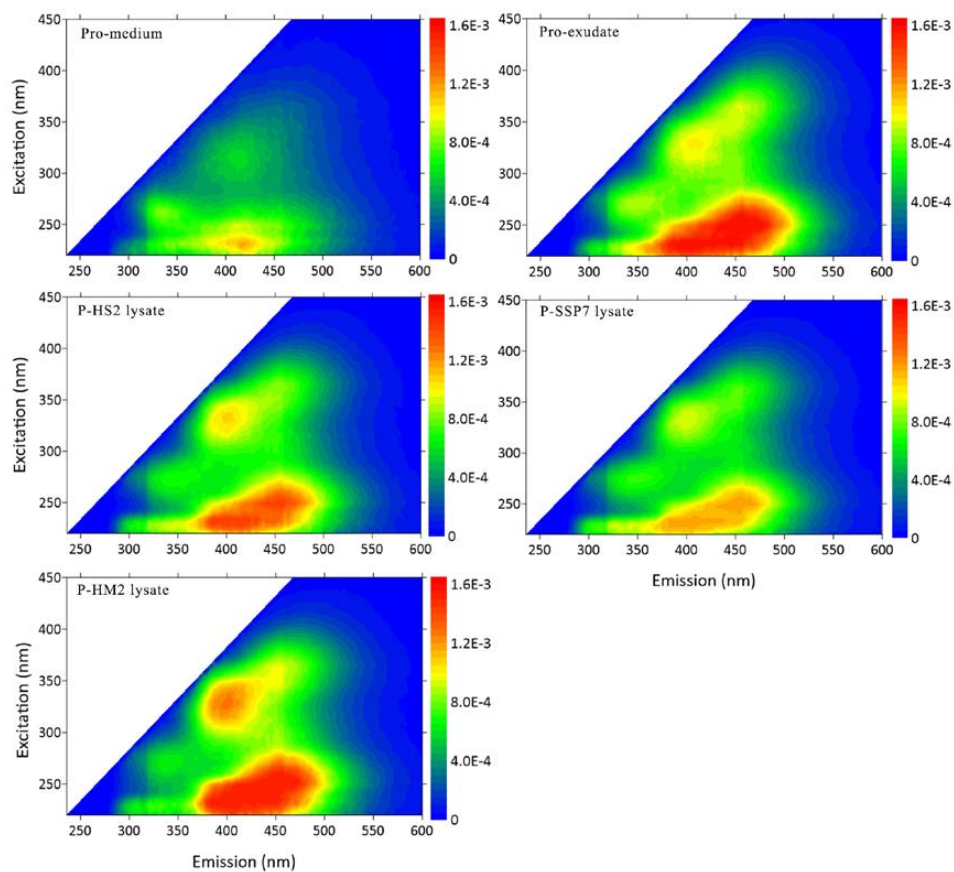
- 694 bioavailability of C, N, P, Se, and Fe following viral lysis of a marine chrysophyte. *Limnology and*  
695 *Oceanography* 42:1492-1504.
- 696 17. Jiao N, Herndl GJ, Hansell DA, Benner R, Kattner G, Wilhelm SW, Kirchman DL, Weinbauer MG,  
697 Luo TW, Chen F, Azam F. 2010. Microbial production of recalcitrant dissolved organic matter:  
698 long-term carbon storage in the global ocean. *Nature Reviews Microbiology* 8:593-599.
- 699 18. Azam F, Fenchel T, Field JG, Gray JS, Meyerreil LA, Thingstad F. 1983. The Ecological Role of  
700 Water-Column Microbes in the Sea. *Marine Ecology Progress Series* 10:257-263.
- 701 19. Haaber J, Middelboe M. 2009. Viral lysis of *Phaeocystis pouchetii*: Implications for algal  
702 population dynamics and heterotrophic C, N and P cycling. *ISME J* 3:430-441.
- 703 20. Sheik AR, Brussaard CPD, Lavik G, Lam P, Musat N, Krupke A, Littmann S, Strous M, Kuypers  
704 MMM. 2014. Responses of the coastal bacterial community to viral infection of the algae  
705 *Phaeocystis globosa*. *Isme Journal* 8:212-225.
- 706 21. Fang X, Liu Y, Zhao Y, Chen Y, Liu R, Qin Q-L, Li G, Zhang Y-Z, Chan W, Hess WR, Zeng Q. 2019.  
707 Transcriptomic responses of the marine cyanobacterium *Prochlorococcus* to viral lysis products.  
708 *Environmental Microbiology* 21:2015-2028.
- 709 22. Flombaum P, Gallegos JL, Gordillo RA, Rincon J, Zabala LL, Jiao NAZ, Karl DM, Li WKW, Lomas  
710 MW, Veneziano D, Vera CS, Vrugt JA, Martiny AC. 2013. Present and future global distributions  
711 of the marine Cyanobacteria *Prochlorococcus* and *Synechococcus*. *Proceedings of the National*  
712 *Academy of Sciences of the United States of America* 110:9824-9829.
- 713 23. Partensky F, Garczarek L. 2010. *Prochlorococcus*: Advantages and Limits of Minimalism. *Annual*  
714 *Review of Marine Science* 2:305-331.
- 715 24. Pasulka AL, Samo TJ, Landry MR. 2015. Grazer and viral impacts on microbial growth and  
716 mortality in the southern California Current Ecosystem. *Journal of Plankton Research* 37:320-  
717 336.
- 718 25. Baudoux AC, Veldhuis MJW, Witte HJ, Brussaard CPD. 2007. Viruses as mortality agents of  
719 picophytoplankton in the deep chlorophyll maximum layer during IRONAGES III. *Limnology and*  
720 *Oceanography* 52:2519-2529.
- 721 26. Lea-Smith DJ, Biller SJ, Davey MP, Cotton CAR, Sepulveda BMP, Turchyn AV, Scanlan DJ, Smith  
722 AG, Chisholm SW, Howe CJ. 2015. Contribution of cyanobacterial alkane production to the  
723 ocean hydrocarbon cycle. *Proceedings of the National Academy of Sciences of the United*  
724 *States of America* 112:13591-13596.
- 725 27. Becker JW, Berube PM, Follett CL, Waterbury JB, Chisholm SW, DeLong EF, Repeta DJ. 2014.  
726 Closely related phytoplankton species produce similar suites of dissolved organic matter.  
727 *Frontiers in Microbiology* 5.
- 728 28. Bouman HA, Ulloa O, Scanlan DJ, Zwirgmaier K, Li WKW, Platt T, Stuart V, Barlow R, Leth O,  
729 Clementson L, Lutz V, Fukasawa M, Watanabe S, Sathyendranath S. 2006. Oceanographic basis  
730 of the global surface distribution of *Prochlorococcus* ecotypes. *Science* 312:918-921.
- 731 29. Hansen AM, Kraus TEC, Pellerin BA, Fleck JA, Downing BD, Bergamaschi BA. 2016. Optical  
732 properties of dissolved organic matter (DOM): Effects of biological and photolytic degradation.  
733 *Limnology and Oceanography* 61:1015-1032.
- 734 30. Catalá TS, Álvarez-Salgado XA, Otero J, Luculano F, Companys B, Horstkotte B, Romera-Castillo  
735 C, Nieto-Cid M, Latasa M, Morán XAG, Gasol JM, Marrasé C, Stedmon CA, Reche I. 2016. Drivers  
736 of fluorescent dissolved organic matter in the global epipelagic ocean. *Limnology and*  
737 *Oceanography* 61:1101-1119.

- 738 31. Yamashita Y, Tanoue E. 2008. Production of bio-refractory fluorescent dissolved organic matter  
739 in the ocean interior. *Nature Geoscience* 1:579-582.
- 740 32. Moore LR, Coe A, Zinser ER, Saito MA, Sullivan MB, Lindell D, Frois-Moniz K, Waterbury J,  
741 Chisholm SW. 2007. Culturing the marine cyanobacterium *Prochlorococcus*. *Limnology and*  
742 *Oceanography-Methods* 5:353-362.
- 743 33. Wong GTF, Ku T-L, Mulholland M, Tseng C-M, Wang D-P. 2007. The SouthEast Asian Time-series  
744 Study (SEATS) and the biogeochemistry of the South China Sea—An overview. *Deep Sea*  
745 *Research Part II: Topical Studies in Oceanography* 54:1434-1447.
- 746 34. Docherty KM, Young KC, Maurice PA, Bridgham SD. 2006. Dissolved Organic Matter  
747 Concentration and Quality Influences upon Structure and Function of Freshwater Microbial  
748 Communities. *Microbial Ecology* 52:378-388.
- 749 35. Logue JB, Lindström ES. 2008. Biogeography of Bacterioplankton in Inland Waters. *Freshwater*  
750 *Reviews* 1:99-114.
- 751 36. Sarmiento H, Morana C, Gasol JM. 2016. Bacterioplankton niche partitioning in the use of  
752 phytoplankton-derived dissolved organic carbon: quantity is more important than quality.  
753 *ISME J* 10:2582-2592.
- 754 37. Lindroth P, Mopper K. 1979. High performance liquid chromatographic determination of  
755 subpicomole amounts of amino acids by precolumn fluorescence derivatization with o-  
756 phthaldialdehyde. *Analytical Chemistry* 51:1667-1674.
- 757 38. Li X, Liu Z, Chen W, Wang L, He B, Wu K, Gu S, Jiang P, Huang B, Dai M. 2018. Production and  
758 Transformation of Dissolved and Particulate Organic Matter as Indicated by Amino Acids in the  
759 Pearl River Estuary, China. *Journal of Geophysical Research: Biogeosciences* 123:3523-3537.
- 760 39. Yamashita Y, Cory RM, Nishioka J, Kuma K, Tanoue E, Jaffe R. 2010. Fluorescence characteristics  
761 of dissolved organic matter in the deep waters of the Okhotsk Sea and the northwestern North  
762 Pacific Ocean. *Deep-Sea Research Part II-Topical Studies in Oceanography* 57:1478-1485.
- 763 40. Spencer RGM, Hernes PJ, Ruf R, Baker A, Dyda RY, Stubbins A, Six J. 2010. Temporal controls on  
764 dissolved organic matter and lignin biogeochemistry in a pristine tropical river, Democratic  
765 Republic of Congo. *Journal of Geophysical Research: Biogeosciences* 115:n/a-n/a.
- 766 41. Guo W, Yang L, Zhai W, Chen W, Osburn CL, Huang X, Li Y. 2014. Runoff-mediated seasonal  
767 oscillation in the dynamics of dissolved organic matter in different branches of a large  
768 bifurcated estuary—The Changjiang Estuary. *Journal of Geophysical Research: Biogeosciences*  
769 119:776-793.
- 770 42. Helms JR, Stubbins A, Ritchie JD, Minor EC, Kieber DJ, Mopper K. 2008. Absorption spectral  
771 slopes and slope ratios as indicators of molecular weight, source, and photobleaching of  
772 chromophoric dissolved organic matter. *Limnology and Oceanography* 53:955-969.
- 773 43. Stedmon CA, Bro R. 2008. Characterizing dissolved organic matter fluorescence with parallel  
774 factor analysis: a tutorial. *Limnology and Oceanography-Methods* 6:572-579.
- 775 44. Coble PG. 1996. Characterization of marine and terrestrial DOM in seawater using excitation  
776 emission matrix spectroscopy. *Marine Chemistry* 51:325-346.
- 777 45. Marie D, Partensky F, Vaultot D, Brussaard C. 1999. Enumeration of Phytoplankton, Bacteria,  
778 and Viruses in Marine Samples. *Current Protocols in Cytometry* 10:11.11.1-11.11.15.
- 779 46. Zhang R, Xia X, Lau SCK, Motegi C, Weinbauer MG, Jiao N. 2013. Response of bacterioplankton  
780 community structure to an artificial gradient of  $p\text{CO}_2$  in the Arctic Ocean. *Biogeosciences*  
781 10:3679-3689.

- 782 47. Klindworth A, Pruesse E, Schweer T, Peplies J, Quast C, Horn M, Glöckner FO. 2013. Evaluation  
783 of general 16S ribosomal RNA gene PCR primers for classical and next-generation sequencing-  
784 based diversity studies. *Nucleic Acids Research* 41:e1-e1.
- 785 48. Magoč T, Salzberg SL. 2011. FLASH: fast length adjustment of short reads to improve genome  
786 assemblies. *Bioinformatics* 27:2957-2963.
- 787 49. Caporaso JG, Kuczynski J, Stombaugh J, Bittinger K, Bushman FD, Costello EK, Fierer N, Peña AG,  
788 Goodrich JK, Gordon JI, Huttley GA, Kelley ST, Knights D, Koenig JE, Ley RE, Lozupone CA,  
789 McDonald D, Muegge BD, Pirrung M, Reeder J, Sevinsky JR, Turnbaugh PJ, Walters WA,  
790 Widmann J, Yatsunenko T, Zaneveld J, Knight R. 2010. QIIME allows analysis of high-throughput  
791 community sequencing data. *Nature Methods* 7:335.
- 792 50. Edgar RC, Haas BJ, Clemente JC, Quince C, Knight R. 2011. UCHIME improves sensitivity and  
793 speed of chimera detection. *Bioinformatics* 27:2194-2200.
- 794 51. Edgar RC. 2013. UPARSE: highly accurate OTU sequences from microbial amplicon reads.  
795 *Nature Methods* 10:996.
- 796 52. Wang Q, Garrity GM, Tiedje JM, Cole JR. 2007. Naïve Bayesian Classifier for Rapid Assignment  
797 of rRNA Sequences into the New Bacterial Taxonomy. *Applied and Environmental Microbiology*  
798 73:5261-5267.
- 799 53. DeSantis TZ, Hugenholtz P, Larsen N, Rojas M, Brodie EL, Keller K, Huber T, Dalevi D, Hu P,  
800 Andersen GL. 2006. Greengenes, a Chimera-Checked 16S rRNA Gene Database and Workbench  
801 Compatible with ARB. *Applied and Environmental Microbiology* 72:5069-5072.
- 802 54. Barberán A, Bates ST, Casamayor EO, Fierer N. 2011. Using network analysis to explore co-  
803 occurrence patterns in soil microbial communities. *The ISME Journal* 6:343.
- 804 55. Yamashita Y, Panton A, Mahaffey C, Jaffé R. 2011. Assessing the spatial and temporal variability  
805 of dissolved organic matter in Liverpool Bay using excitation–emission matrix fluorescence and  
806 parallel factor analysis. *Ocean Dynamics* 61:569-579.
- 807 56. Kothawala DN, von Wachenfeldt E, Koehler B, Tranvik LJ. 2012. Selective loss and preservation  
808 of lake water dissolved organic matter fluorescence during long-term dark incubations. *Science*  
809 *of The Total Environment* 433:238-246.
- 810 57. Shen Y, Fichot CG, Benner R. 2012. Dissolved organic matter composition and bioavailability  
811 reflect ecosystem productivity in the Western Arctic Ocean. *Biogeosciences* 9:4993-5005.
- 812 58. Bianchi TS, Thornton DCO, Yvon-Lewis SA, King GM, Eglinton TI, Shields MR, Ward ND, Curtis J.  
813 2015. Positive priming of terrestrially derived dissolved organic matter in a freshwater  
814 microcosm system. *Geophysical Research Letters* 42:5460-5467.
- 815 59. Wilhelm SW, Suttle CA. 1999. Viruses and Nutrient Cycles in the Sea - Viruses play critical roles  
816 in the structure and function of aquatic food webs. *Bioscience* 49:781-788.
- 817 60. Landa M, Blain S, Harmand J, Monchy S, Rapaport A, Obernosterer I. 2018. Major changes in  
818 the composition of a Southern Ocean bacterial community in response to diatom-derived  
819 dissolved organic matter. *FEMS Microbiology Ecology* 94:fiy034-fiy034.
- 820 61. Tada Y, Suzuki K. 2016. Changes in the community structure of free-living heterotrophic  
821 bacteria in the open tropical Pacific Ocean in response to microalgal lysate-derived dissolved  
822 organic matter. *FEMS Microbiology Ecology* 92.
- 823 62. Zhang R, Weinbauer M, Tam Y, Qian P-Y. 2013. Response of bacterioplankton to a glucose  
824 gradient in the absence of lysis and grazing. *FEMS microbiology ecology* 85.
- 825 63. Thompson LR, Zeng Q, Kelly L, Huang KH, Singer AU, Stubbe J, Chisholm SW. 2011. Phage

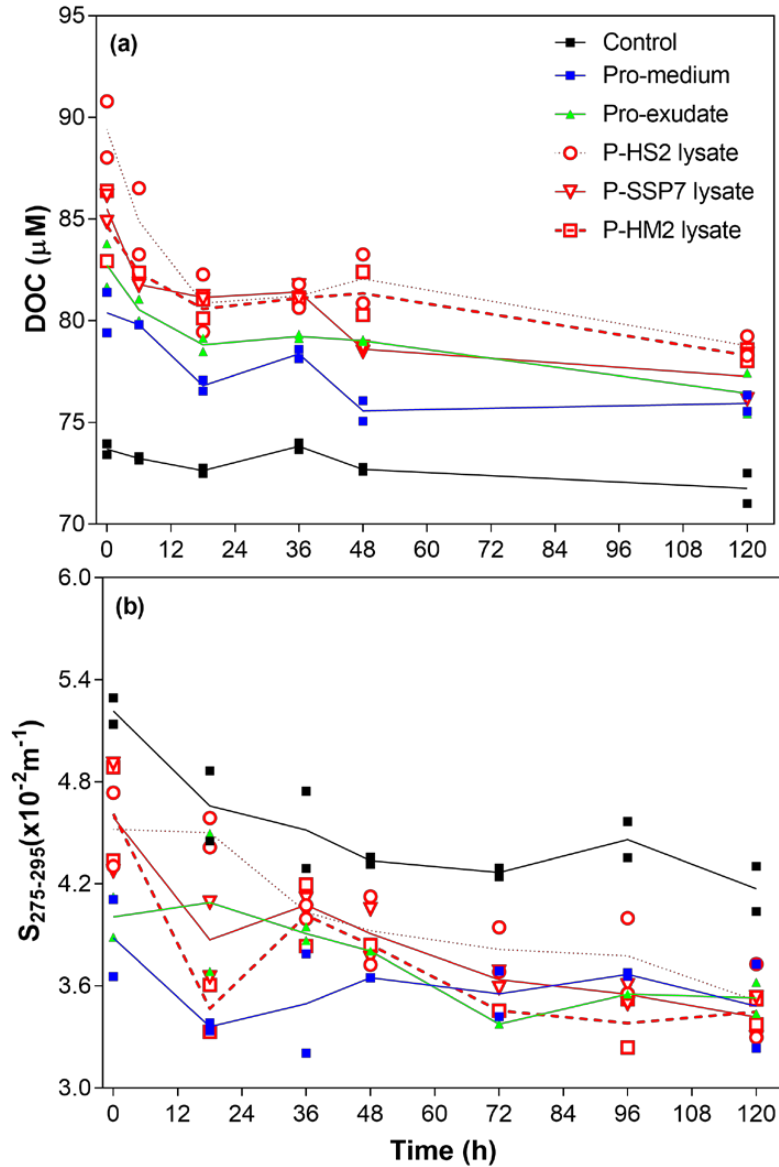
- 826 auxiliary metabolic genes and the redirection of cyanobacterial host carbon metabolism.  
827 Proceedings of the National Academy of Sciences of the United States of America 108:E757-  
828 E764.
- 829 64. Frois-Moniz K. 2014. Host/Virus Interactions in the Marine Cyanobacterium *Prochlorococcus*.  
830 Ph.D Thesis. Massachusetts Institute of Technology, Cambridge, MA.
- 831 65. Nelson CE, Carlson CA. 2012. Tracking differential incorporation of dissolved organic carbon  
832 types among diverse lineages of Sargasso Sea bacterioplankton. *Environmental Microbiology*  
833 14:1500-1516.
- 834 66. Taylor JD, Cunliffe M. 2017. Coastal bacterioplankton community response to diatom-derived  
835 polysaccharide microgels. *Environmental Microbiology Reports* 9:151-157.
- 836 67. Gómez-Consarnau L, Lindh MV, Gasol JM, Pinhassi J. 2012. Structuring of bacterioplankton  
837 communities by specific dissolved organic carbon compounds. *Environmental Microbiology*  
838 14:2361-2378.
- 839 68. Ogawa H, Amagai Y, Koike I, Kaiser K, Benner R. 2001. Production of refractory dissolved organic  
840 matter by bacteria. *Science* 292:917-920.
- 841 69. Fasching C, Behounek B, Singer GA, Battin TJ. 2014. Microbial degradation of terrigenous  
842 dissolved organic matter and potential consequences for carbon cycling in brown-water  
843 streams. *Scientific Reports* 4:4981.
- 844 70. Faust K, Raes J. 2012. Microbial interactions: from networks to models. *Nature Reviews*  
845 *Microbiology* 10:538.
- 846 71. Martínez-Pérez AM, Catalá TS, Nieto-Cid M, Otero J, Álvarez M, Emelianov M, Reche I, Álvarez-  
847 Salgado XA, Aristegui J. 2019. Dissolved organic matter (DOM) in the open Mediterranean Sea.  
848 II: Basin-wide distribution and drivers of fluorescent DOM. *Progress in Oceanography* 106:93-  
849 106.
- 850 72. Biller SJ, Berube PM, Lindell D, Chisholm SW. 2015. *Prochlorococcus*: the structure and function  
851 of collective diversity. *Nature Reviews Microbiology* 13:13-27.
- 852 73. Catalá TS, Reche I, Fuentes-Lema A, Romera-Castillo C, Nieto-Cid M, Ortega-Retuerta E, Calvo  
853 E, Alvarez M, Marrase C, Stedmon CA, Alvarez-Salgado XA. 2015. Turnover time of fluorescent  
854 dissolved organic matter in the dark global ocean. *Nature Communications* 6.
- 855 74. Kaplan A. 2016. Cyanophages: Starving the Host to Recruit Resources. *Current Biology* 26:R511-  
856 R513.
- 857 75. Hurwitz BL, U'Ren JM. 2016. Viral metabolic reprogramming in marine ecosystems. *Current*  
858 *Opinion in Microbiology* 31:161-168.
- 859 76. Sharma AK, Becker JW, Ottesen EA, Bryant JA, Duhamel S, Karl DM, Cordero OX, Repeta DJ,  
860 DeLong EF. 2014. Distinct dissolved organic matter sources induce rapid transcriptional  
861 responses in coexisting populations of *Prochlorococcus*, *Pelagibacter* and the OM60 clade.  
862 *Environmental Microbiology* 16:2815-2830.
- 863 77. Dadaglio L, Dinasquet J, Obernosterer I, Joux F. 2018. Differential responses of bacteria to  
864 diatom-derived dissolved organic matter in the Arctic Ocean. *Aquatic Microbial Ecology* 82:59-  
865 72.
- 866 78. Jürgens K, Gasol JM, Vaqué D. 2000. Bacteria–flagellate coupling in microcosm experiments in  
867 the Central Atlantic Ocean. *Journal of Experimental Marine Biology and Ecology* 245:127-147.
- 868 79. Zhang R, Weinbauer MG, Qian P-Y. 2007. Viruses and flagellates sustain apparent richness and  
869 reduce biomass accumulation of bacterioplankton in coastal marine waters. *Environmental*

- 870 Microbiology 9:3008-3018.
- 871 80. Gasol J, M. , Morán X, A. G. 1999. Effects of filtration on bacterial activity and picoplankton  
872 community structure as assessed by flow cytometry. *Aquatic Microbial Ecology* 16:251-264.
- 873 81. Bertilsson S, Berglund O, Karl DM, Chisholm SW. 2003. Elemental composition of marine  
874 *Prochlorococcus* and *Synechococcus*: Implications for the ecological stoichiometry of the sea.  
875 *Limnology and Oceanography* 48:1721-1731.
- 876

877 **Figures**

878

879 Figure 1. Viral lysis enhanced the production of fluorescent DOM derived from  
880 *Prochlorococcus*. The fluorescence intensity of the excitation-emission matrix of the  
881 five generated DOM were normalized to the DOC concentration. Unit:  $L \mu\text{mol-C}^{-1}$  R.U.  
882 The scale bar along each figure represents the fluorescence intensity. Please note the  
883 scale bar differences between different graphs.



884

885 Figure 2. Changes in DOM quantity and quality after incubation with *Prochlorococcus*

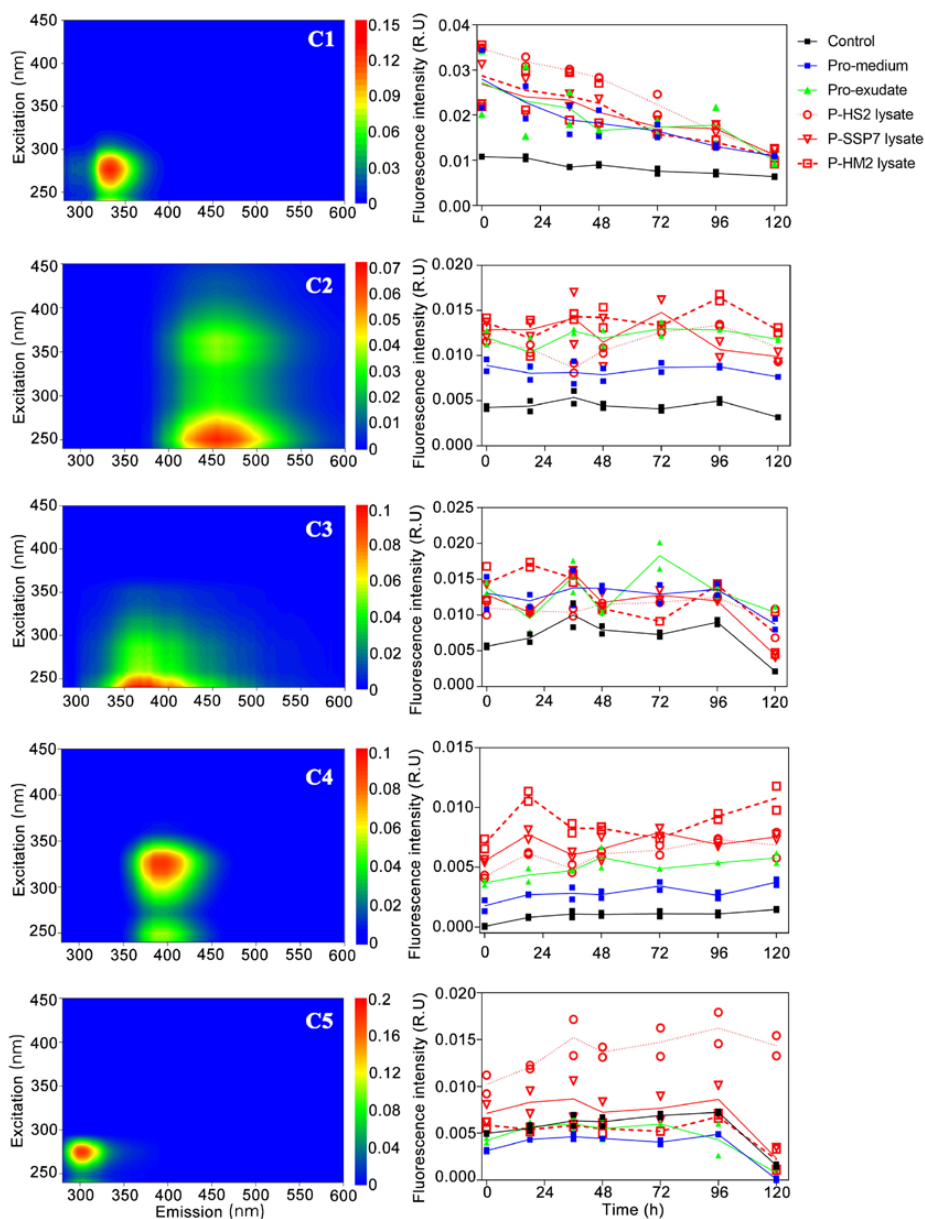
886 exudate and lysate produced by different viruses. (a) Microbial utilization of different

887 DOC derived from *Prochlorococcus* DOM; (b) the DOM spectral slope  $S_{275-295}$ , which is

888 typically related to DOM molecular weight, at specific sampling times for each DOM

889 treatment. The value of each replicate and the trend line of each treatment are shown.



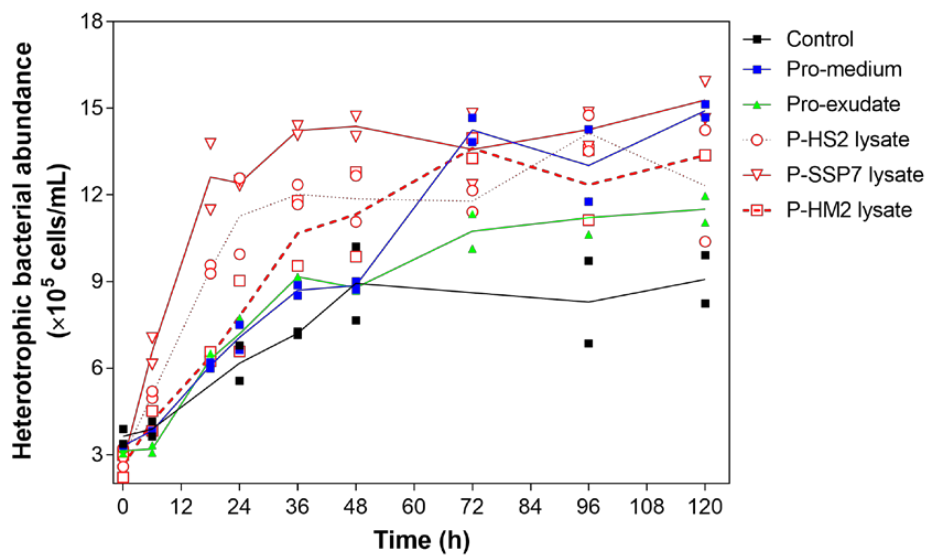


890

891 Figure 3. Microbial utilization of different components of fluorescent DOM derived  
 892 from *Prochlorococcus*. Left panels, excitation-emission matrix contours of the five  
 893 fluorescent components (C1-C5) identified using PARAFAC analysis; right panels, the  
 894 corresponding FDOM component changed after incubation with different types of  
 895 *Prochlorococcus*-derived DOM. The value of each replicate and the trend line of each

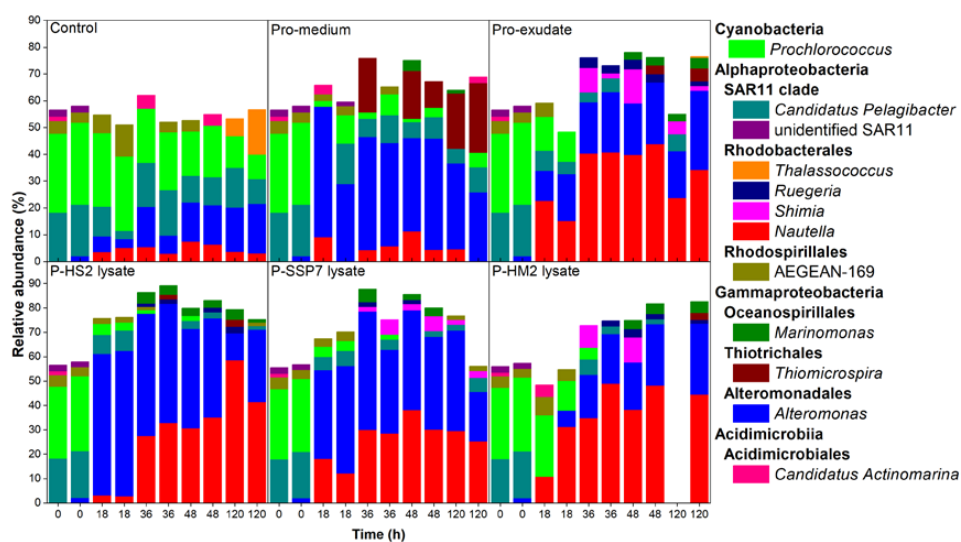


896 treatment are shown.



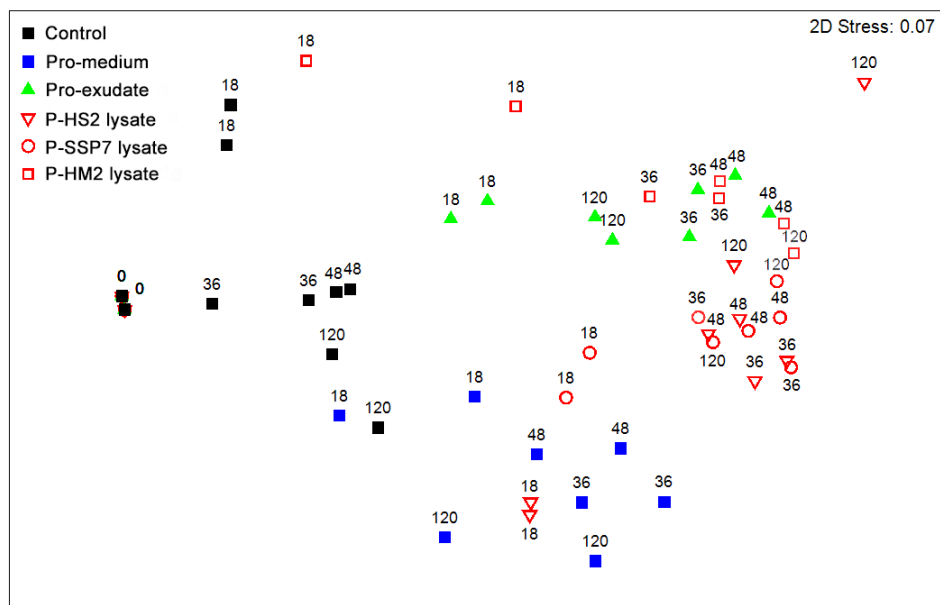
897

898 Figure 4. Growth of heterotrophic bacterioplankton after incubation with  
899 *Prochlorococcus*-derived DOM. The value of each replicate and the trend line of each  
900 treatment are shown.



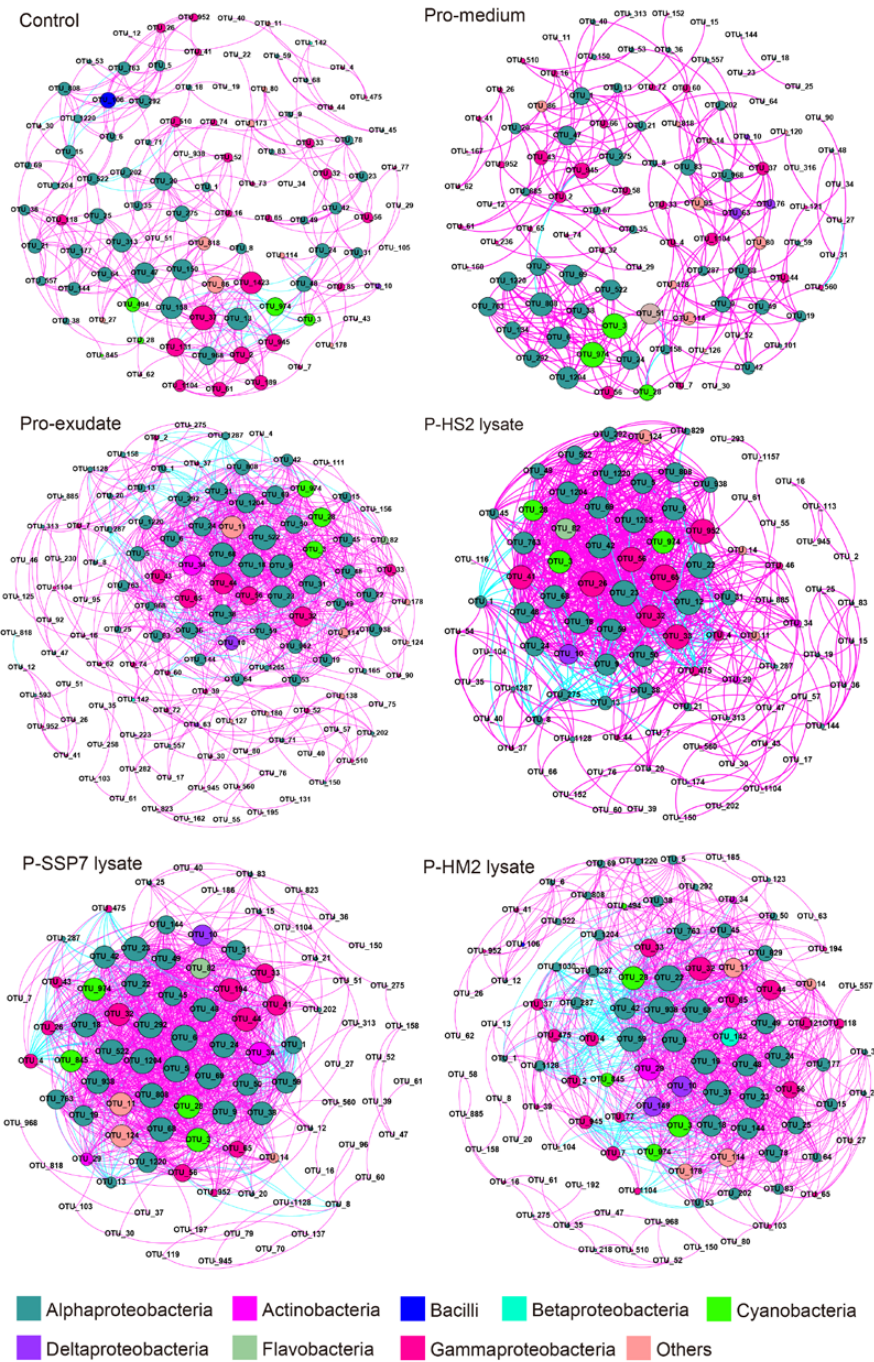
901

902 Figure 5. The response of the microbial community structure (genus level) to  
 903 *Prochlorococcus*-derived DOM. The top 5 abundant genera in at least one sample were  
 904 selected. Two bars having the same x-axis indicates replicates, and two replicates of  
 905 each Pro-DOM treatment at each sampling time data are shown here (except the P-  
 906 HM2 lysate at 120 h, which had only one sample). The names of the treatments are  
 907 shown in the corresponding figures.



908

909 Figure 6. Effect of *Prochlorococcus*-derived DOM on the succession of the bacterial  
 910 community structure, as revealed by nonmetric multidimensional scaling (NMDS)  
 911 analysis. The number on each symbol indicates the sampling time of each treatment,  
 912 and all treatments at each sampling time had two replicates (except the P-HM2 lysate  
 913 treatment at 120 h), as shown by two of each symbol having the same number.

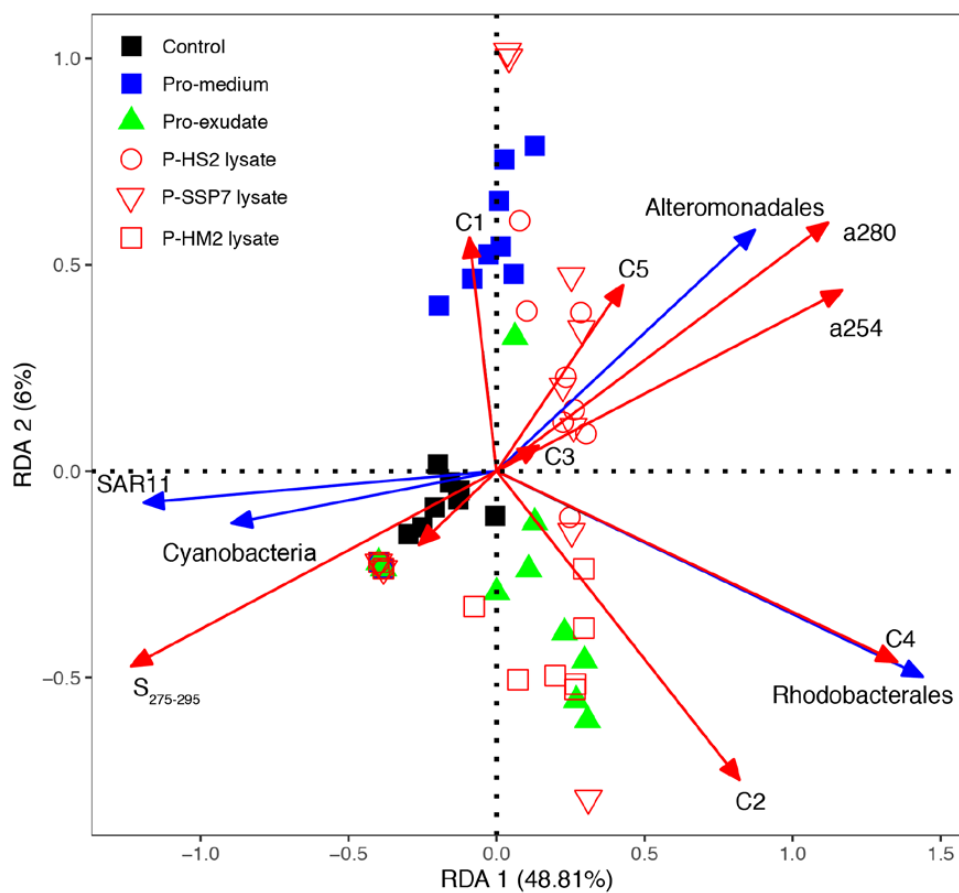


914

915 Figure 7. OTU-based network revealing intense interaction among microbial

916 communities after incubation with *Prochlorococcus*-derived DOM. Red and cyan

917 connections represent positive and negative interactions, respectively.



918

919 Figure 8. Redundancy analysis illustrating specific bacterial groups closely linked to

920 specific DOM characteristics.  $a_{280}$ , C2, C5,  $P = 0.001$ ; C4,  $P = 0.01$ ;  $S_{275-295}$ , C3,  $p < 0.05$ ;921 DOC, C1,  $a_{254}$ ,  $P > 0.05$ . Only the bacterial groups that were significantly correlated with

922 DOM indices are shown in the figure. All the bacterial community samples (without

923 sampling times) are also presented in the figure. The samples located on the positive

924 section of the second axis of the RDA figure are the early samples (at 18 or 36 h) of

925 this incubation.

926 **Tables**

927 Table 1. The DOC concentration and optical properties of the DOM derived from *Prochlorococcus*. The FDOM components (C1-C5), as identified by  
 928 PARAFAC modelling, are shown with the corresponding FDOM components (peaks A, M, C and T) identified by the peak-picking method. The data  
 929 shown are the means of two replicates.

DOM source	DOC ( $\mu\text{M}$ )	$a_{254}$ ( $\text{m}^{-1}$ )	$S_{275-295}^*$ ( $10^{-2} \text{ nm}^{-1}$ )	Humic like components (R.U.)						Protein like components (R.U.)		
				peak A 250/466	C2 255/456	peak M * 335/404	C4 * 325/396	peak C 355/450	C3 <250/368	peak T 270/342	C1 275/332	C5 275/300
Pro-medium	160.9	-	-	0.19	0.12	0.09	0.08	0.06	0.13	0.15	0.13	0.04
Pro-exudate	234.0	3.37	2.88	0.36	0.36	0.22	0.22	0.20	0.19	0.25	0.24	0.08
P-HS2 lysate	259.5	3.65	3.29	0.37	0.34	0.27	0.26	0.21	0.14	0.19	0.18	0.08
P-SSP7 lysate	319.0	4.77	4.27	0.35	0.36	0.29	0.28	0.23	0.18	0.26	0.26	0.08
P-HM2 lysate	244.4	5.08	3.80	0.38	0.38	0.30	0.30	0.22	0.17	0.19	0.19	0.06

930 \*, represent the significant difference between Pro-exudate and Pro-vDOM, t-test (double tailed),  $P < 0.05$ .